SELF-SIMILAR BEHAVIOUR OF CPI HEADLINE INFLATION

Authors

D. Mallikarjuna Reddy
Department of Mathematics
Gitam University
Hyderabad, Telangana, India.
drmallikreddyd@gmail.com

Thandu Vamshi Krishna
Department of Mathematics
Gitam University
Hyderabad, Telangana, India.
vthandu556@gmail.com

I. INTRODUCTION

Core inflation has a significant role in monetary policy decisions. Core inflation is determined by removing the temporary price changes and retaining permanent (core) price changes of the headline inflation commodity basket. Forecasting inflation is of vital interest to policymakers. Different methodologies are constructed for measuring core inflation like exclusion based method, symmetric trim method, asymmetric trim method, weighted median method, and moving average process. The inflation, a time series, was estimated by applying the ARIMA model (Iqbal et al., 2016; Habibah et al., 2017). Long memory properties of inflation are studied globally, and ARFIMA models are suggested (Hassler & Wolters, 1995; Baillie & Morano, 2012). In this study, we concentrate on the characteristics of the headline and core inflation rather than the methods to determine the core inflation. Various properties of core inflation are presented in the literature (Marques, 2003). Previous studies reported the presence of LRD behaviour in the inflation of some countries. Inspired by these facts, we examined India's monthly CPI headline inflation to check the self-similarity. Besides that, we try to identify whether the headline inflation series belong to SRD or LRD based on the Hurst exponent. The current study to compute the Hurst index is based on different approaches methods like the R/S method, Variance-Time method, Higuchi's method and Average Periodogram method. The Hurst parameter estimate gives an idea about the strength of the self-similar nature in CPI headline inflation of India. The chapter presents a criteria for core inflation measures in terms of Hurst exponent. Then core inflation indicators for CPI inflation are selected based on the exclusion approach and examined their Hurst exponents along with other properties of core inflation for the possibility of being a core inflation measure. The present study plays a prominent role in the determination of core inflation in the Indian context. The empirical investigation has been conducted using monthly Combined CPI time series data considering the period: Jan 2012-April 2019 (base year: 2012). The CPI headline Y-o-Y inflation is computed and checked for the self-similarity behaviour by computing Hurst exponent. R programming and MS Excel tools are used for performing the analysis.

The remaining work of the chapter has been planned as follows: Section 2.2 presents the overview of the time series concepts. Section 2.3 discusses the preliminaries of self-similarity, its definition and usage in various fields. Section 2.4 offers the literature review in the context of self-similarity applications. Section 2.5 discusses the different methods to compute the Hurst exponent. Section 2.6 presents the numerical results of the Hurst exponent for the CPI headline inflation. Section 2.7 establishes new criteria for core inflation based on the Hurst exponent and applies it to the conventional CPI exclusion measures. Section 2.9 presents the conclusions of the chapter.

II. AN OVERVIEW OF TIME SERIES CONCEPTS

1. **Definition of Time Series:** Time series is a sequence of observations collected in chronological arrangement. A discrete-time time series is obtained when observations are collected at a discrete set of times. It is commonly denoted by $\{X_t\}$, $t\epsilon\{t_1, t_2, \ldots, t_n\}$ where $t_1, t_2, \ldots, t_n$ are the time points at which the random variable X_t is measured. Here 't' can be years, months, weeks, days, hours and even seconds. If the observations of X_t are collected continuously over an interval of time (T), it results in continuous-time time series and denoted by $\{X_t, t\epsilon T\}$. Price of onion in a city collected daily, Number of active covid-19 positive patients in a town collected weekly, Population of Telangana in every census are some of the examples of discrete-time time series. The temperature in a city, Water level of a dam, Velocity of an aeroplane, A continuous-time binary process are some of the examples of continuous-time time series. The dimension of the time series depends on the dimension of the random variable $\{X_t\}$.

   Figure 1 presents the time series plot of the monthly price index for 'sugar and confectionery' of CPI-India data. We can observe the prices of 'sugar and confectionery' increase for some period and then decrease. Fig. 2 presents the time series plot of the monthly price index for 'vegetables' of CPI-India data. Here we can observe some periodicity in prices of 'vegetables,' i.e. the month or season of the year seem to influence the prices.

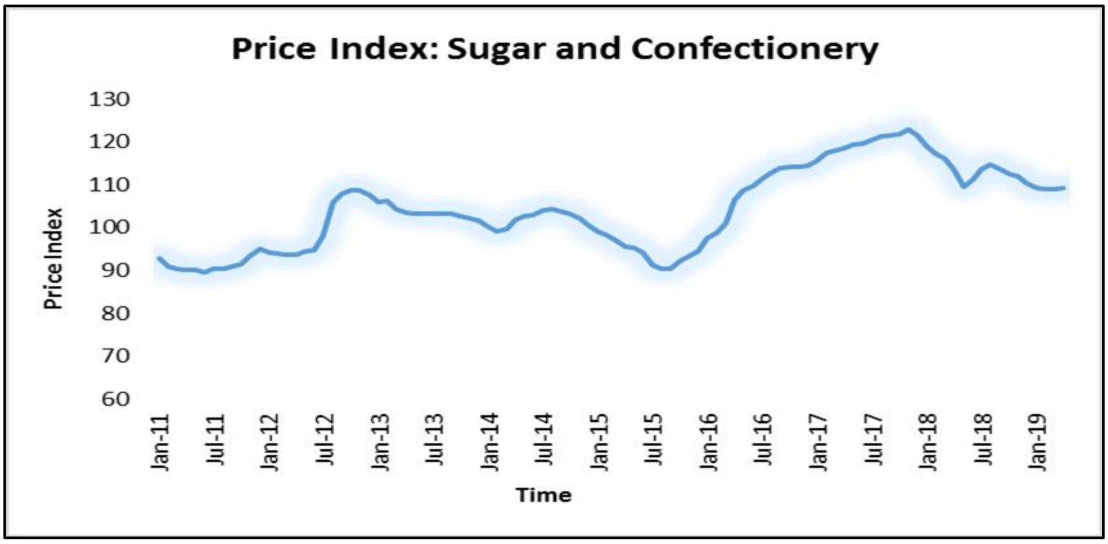

Figure 1: Time series plot of the monthly price index for Sugar and confectionery of CPI-India data

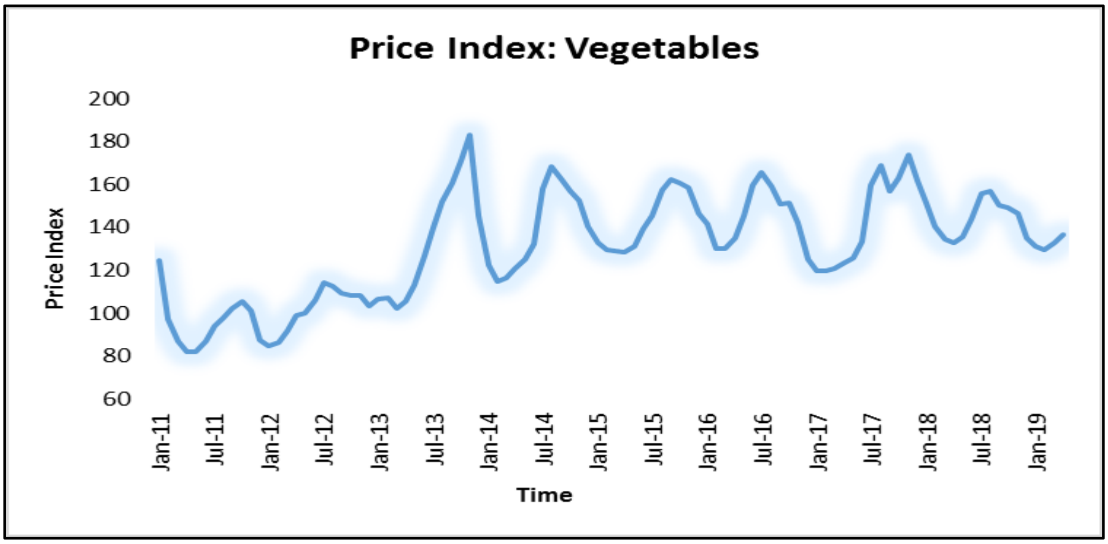

Figure 2: Time series plot of the monthly price index for vegetables of CPI-India data

2. **Components of Time Series:** The various influences that cause the fluctuations in a time series are broadly classified into four categories, usually known as time series components. They are Trend, Seasonal, Cyclic and Irregular or Random variations. These four components are briefly described below. When observed for a long period, the characteristic revealed by time series to rise or decline is termed as a trend. For example, population growth, literacy rate, and monthly family expenditure show an upward trend, whereas mortality rates and labour force engaged in agriculture show a downward trend. It need not be in a unique direction for the total period.

Seasonal variations are periodic in nature and repeatedly occur in regular intervals of time within a period of one year or less. The seasonal variations arise mainly due to natural (climate and weather conditions) and humanmade conventions (festivals, conventions, customary practices etc.). Deals of air coolers, ice cream rise in a warm season, demand for gold ornaments raise in festivals, marriage seasons.

Cyclical variations are also periodic in nature and consist of oscillatory movements (up and down). Cyclical variations extend above a long period of time, generally several years; they cannot be predicted to occur with a regular period of times. Cyclical variations may be present in the economic and financial time series data. In general, a business cycle has four phases- i) Prosperity or period of boom ii) Recession iii) Stagnation or Depression iv)Upturn or Recovery.

The fluctuations that are not caused by the trend, seasonal and cyclical variations are called Irregular fluctuations. They are unpredictable and beyond the control of the human hand. Some of the irregular causes of variations are wars, floods, earthquakes etc.

3. **Decomposition of Time Series:** To study the effect of four factors, generally, two decomposition methods are applied in time series.

Additive Model:

$$Z_t = T_t + S_t + C_t + I_t \tag{2.1}$$

Where T_t is the effect of trend, S_t is the effect of seasonal variations, C_t is the effect of cyclic variations, I_t is the effect of random variations observed at time t. In this model, the components are independent of each other.

Multiplicative Model:

$$Z_t = T_t * S_t * C_t * I_t \tag{2.2}$$

This approach does not assume the independence of components or factors.

Time series data is generated in almost all the fields such as economics, business, engineers, geography, meteorology and the social sciences. An example of time series decomposition is shown below in Fig. 3.

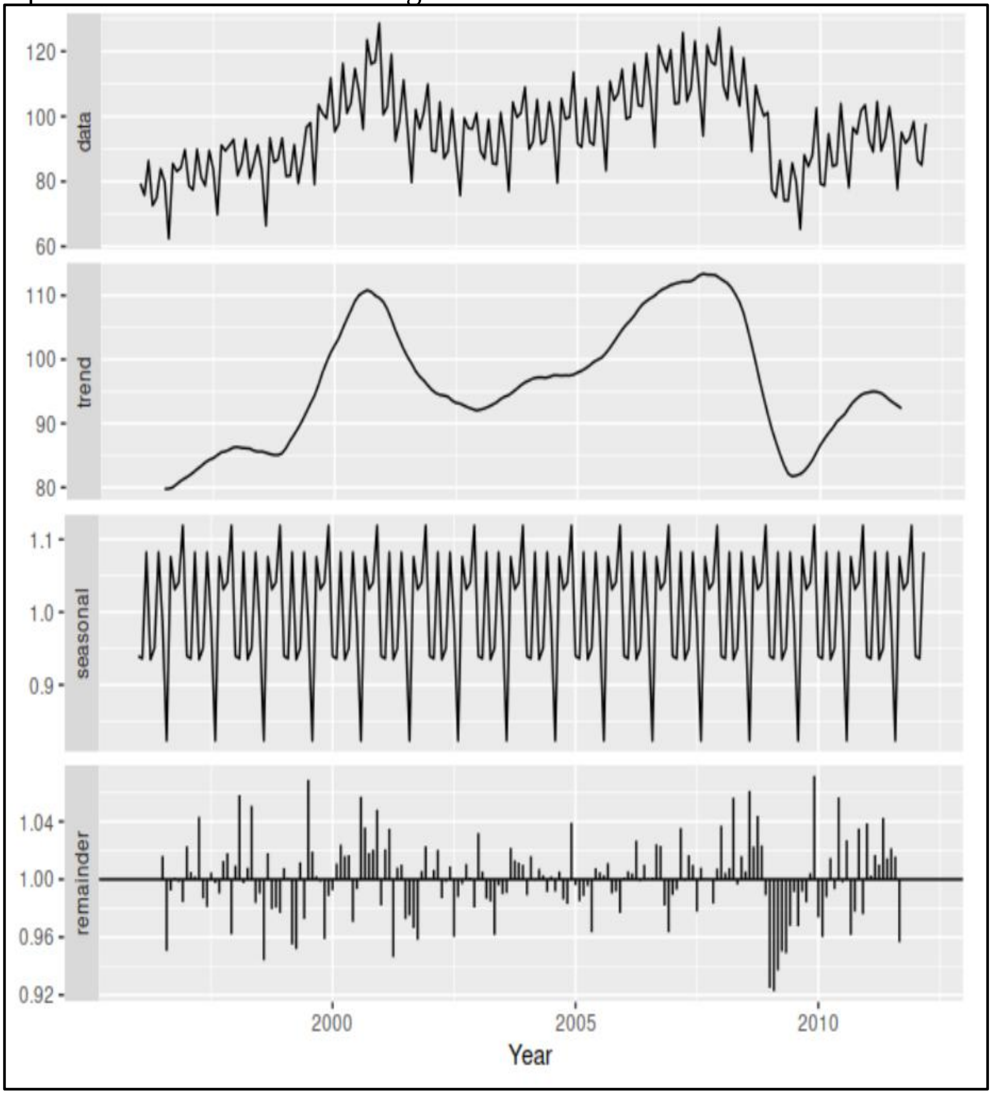

Figure 3: A classical multiplicative decomposition for electrical equipment orders index (United States)

Source: https://otexts.com/fpp2/classical-decomposition.html

4. **Analysis of Time Series:** An essential feature of time series is that consecutive observations are dependent. This dependence among the observations is practically important in any practical situation. The time series analysis commences with the exploration of the dependence within the time-series observations. This involves the development of stochastic and dynamic structure and applications of those models in particular areas (Hipel et al., 1994). Forecasting the future values by using previous and present values using developed models of time series is being the main focus of time series analysis. Fitting a proper time series model is very important, which results in an accurate forecast.

The probabilistic design of a sequence of data points described by a model is called a stochastic process (Cochrane, 1997). An N successive data points $\mathrm{X_1, X_2, ..., X_n}$ from a time series is a sample from the stochastic process. The main desire of statistical analysis is to conjecture the characteristics of the population from the characteristics of the sample. To forecast means to deduce the probabilistic pattern of future values for the population under a specified sample $\{\mathrm{X_t}\}$.

5. **Stationary Process:** A key aspect in the invention of the models of time series is based on a belief that it is of the appearance of statistical stability. In precise, this kind of assumption is stationarity. In general, different stationarity of time series process are defined by its mean, variance and autocorrelation structure or spectral density function.

Definition 2.1: A process $\{\mathrm{X_t}\}$ is the first-order stationary if its pdf doesn't change over time i.e.

$$f_X(x,t) = f_X(x,t+h),\ \forall t,h \tag{2.3}$$

This results in constant mean of $\{\mathrm{X_t}\}$ over time.

Definition 2.2: A process $\{\mathrm{X_t}\}$ is the second-order stationary if first and second degree density function satisfies

$$f_X(x_1,t_1) = f_X(x_1,t_1+h)\ \ \forall t,h \tag{2.4}$$

$$f_X(x_1,x_2,t_1,t_2) = f_X(x_1,x_2,t_1+h,t_2+h)\ \ \forall t_1,t_2,h \tag{2.5}$$

A time-series $\{X_t\}$ is called strictly stationary of order n (n ≥ 1) if the joint probability density function of $\{X_{t_1}, X_{t_2}, \ldots, X_{t_n}\}$ is the same as the joint probability density function of $\{X_{t_1+h}, X_{t_2+h}, ..., X_{t_n+h}\}$, for every value of $t_1, t_2, ..., t_n$, h & n. In other words, if the joint pdf is time-invariant, the time series $\{X_t, t \in T\}$ is strictly stationary.

But in materialistic implementations, the hypothesis of strictly stationary is not necessarily needed; therefore a weekly or second-order or covariance stationarity is considered. A time series is stationary if variance and mean are time-independent. Stationarity in any time series data can be tested by various tests like the Phillips-Perron (PP) test and the Augmented Dickey-Fuller (ADF) test.

In practical applications, time-series data may be non-stationary. As per Hipel and McLeod, as the time span of time series observations increases, the chance of non-stationarity of time series increases. When the data is not stationary, it is to be converted to stationary by stabilizing variance and mean of the series. Preferably variance to be stabilized first and then stabilize means. The variance of a time series can be stabilized by using square root or logarithmic transformations successively. The mean of a data can be made stable by successive differencing. It is to be noted that one observation will be lost in each differencing. It usually requires one or two differencing to stabilize the mean. By stabilizing mean we eliminate the trend in the data. Sometimes seasonal patterns may also be present in the experimental data. Seasonal patterns may be removed by using seasonal differencing. If there are s seasons in a year, then $Y_t = X_t - X_{t-s}$. Generally, there will be twelve seasons for monthly data and four seasons for quarterly data.

The stationarity condition also states that the covariance of X_t, X_{t+k} segregated by k time intervals should be the same for all t. The covariance between X_t and X_{t+k} for lag k is called the autocovariance of lag k and is given by

$$\gamma_k = cov(X_t, X_{t+k}) = E[(X_t - \mu)(X_{t+k} - \mu)] \qquad (2.6)$$

The detailed discussion on ACF and ACVFs are presented in Chapter-IV.

III. SELF-SIMILARITY

In this section, we started with the preliminaries of self-similarity. In the primary segment, we commence the concept of self-similarity by presenting various examples. The Occurrence of self-similarity in nature is discussed widely. The importance of self-similarity and its usefulness in modelling internet traffic data is discussed. Mathematical definitions of self-similarity are stated, and the method of identifying the SRD or LRD nature is explained.

1. **Preliminaries of Self-Similarity:** The notion of self-similarity was pioneered by Mandelbrot (1964) and is used in support of modelling Geological and Hydrological problems. Self-similarity is a word that is a convinced attribute of an entity is retained w.r.t scaling in time or/and space. If an entity is self-similar, its elements, as enhanced, bear a resemblance to the whole configuration.

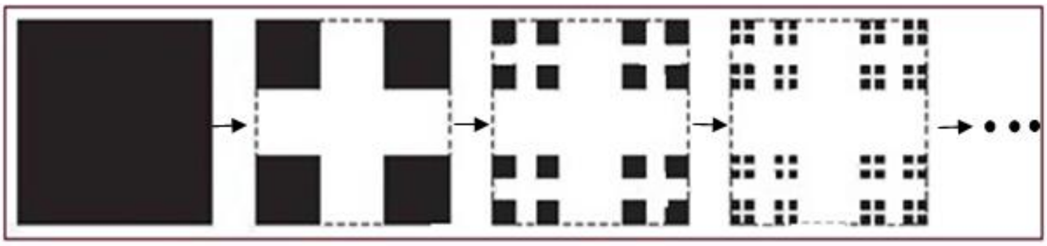

Figure 4: Few stages in the construction of Cantor set

One simple example of self-similarity is the two-dimensional Cantor set which is put up as follows: Consider the set [0, 1] × [0, 1] which is unit square. If each side is trisected, then nine smaller squares are formed. All the squares, except the square at the corners, are to be dropped. Now, the side length of small squares is 1/3 unit. If the same process is repeated to get smaller squares, one obtains a limit set known as the Cantor set.

This construction process of the Cantor set is depicted in Fig. 4. Cantor set has valuable applications in Science and Engineering.

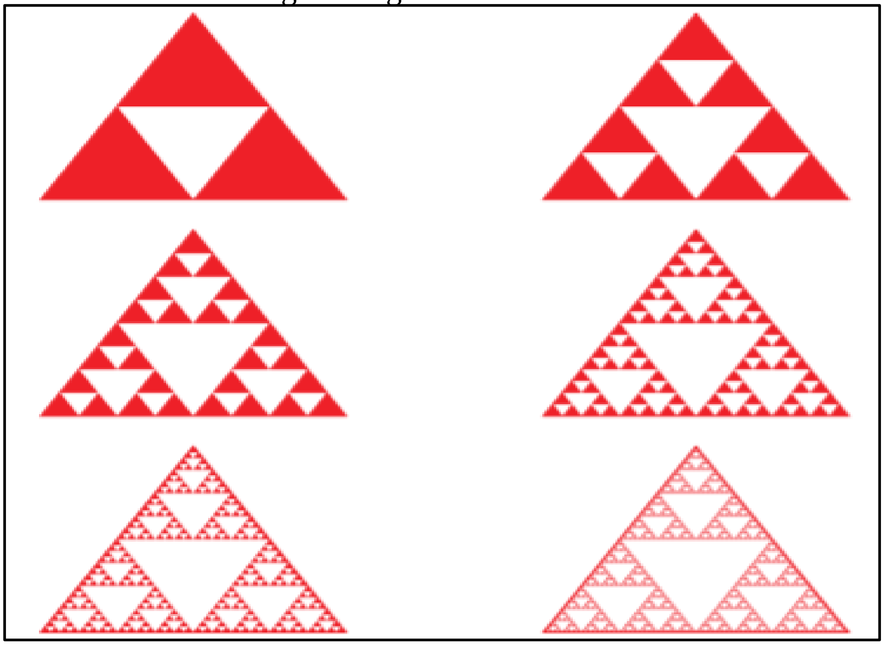

Figure 5: Few stages in the construction of the Sierpinski triangle

Another example of self-similarity is the Sierpinski triangle. Consider an equilateral triangle and identify the midpoints of the sides. Using these points, divide the original equilateral triangle into four congruent triangles. Now, remove the inside triangle and continue dividing each of the remaining three triangles further into four triangles. By continuing the process indefinitely, we get the Sierpinski triangle. This construction process of the Sierpinski triangle is depicted in Fig. 5.

2. **Self-Similarity Screening in Natural World:** In general, self-similarity occurs when the shape of a thing is similar or approximately the same as the part of itself. That is, every portion of the self-similar object is able to consider as a reduced scale of the whole. In natural science, there are a lot of examples of self-similarity, such as fern, snowflake, mountain ridges, coastlines etc. From a view of statistics, self-similarity is defined as two subsets of the whole set are invariant in statistical distribution on different scales. In other words, self-similarity implies being rescaled or translated on the original signal keeps the same statistical distribution.

   As a fresh and exciting topic, many studies on self-similarity have been done in different fields, such as Magneto Hydrodynamics (MHD) in physics, the human nervous system in biology, stellar fragments in astronomy and option pricing in finance etc.

   In historical mathematics, the idea of self-similarity was first introduced (Mandelbrot, 1964). Self-similarity is so broad and plays a significant role in nature, society and arts that it can no longer be computed without as a minimum theoretical indulgence of this barely credible phenomenon. Fortunately, the main thoughts of self-similarity are not so complicated to skilled and illustrations of self-similarity are extraordinarily simple to find out. We can merely understand the fundamentals of self-similar phenomena and be able to recognize them practically everywhere we look.

When graphically mapped, internet traffic provides a striking example of self-similarity in the technological world. In this fractal model, internet hubs (Google and Face book) are represented as the largest nodes on the graphic. Smaller nodes branch off of the major ones, and these represent popular but slightly less travelled sites. And this pattern repeats. At the furthest reaches of the graphic are local networks that receive very little daily traffic. So, basically, based just on graphic representations, our brains, the universe, and the internet are all the same thing.

In the research ground of music information recovery, self-similarity generally refers to the fact that music repeatedly consists of parts that are frequently in time. In other words, music is self-similar under chronological conversion rather than under scaling. In music, strict canons show various amounts of self-similarity, as perform segments of fugues. Sheppard tone is self-similar in the frequency domains.

Romanesco broccoli shows sign of strong self-similarity. Broccoli is another kind of cauliflower. It exhibits strong self-similarity that is a tedious fact. Romanesco broccoli is too possibly the most extremely fractal vegetable in the world. Its pattern absolutely represents spirals upon spirals of the vegetable pattern replicating themselves at various levels of scale.

Figure 6: Dill plant

The Dill plant gives a pleasing and straightforward example of self-similarity with two scales of structure. In the Fig. 6, the main stem goes up to a joint, as of which various secondary stems branch out. Towards the end of every second level stem, there is a small copy through shining third level stems so on present the impressive example of self-similarity. Various categories of cactus plants, for example, the Saguaro, have enlargement patterns turn out a ladder of self-similar lobes.

Having a fairly broad sampling of self-similarity in different areas of nature, make a decision to attempt something new by looking for more conceptual models of this design in common systems, arts and mathematics. If one supposes regarding how our governments, legal systems, different types of economic systems or law enforcement agencies effort one sees that they have quite discrete hierarchical collections with central, state and neighbouring levels frequently being the most important scales. Fundamentally a similar kind of movement is happening at various scales, and thus we discover a well-known design within a new background.

The main characteristic of self-similarity is the same thing on different scales can be obtained in innumerable examples from the social divisions. (Chin Wen Cheong, 2010) proposed the self-similarity through fractionally integrated techniques in financial markets. Self-similarity has vital effects intended for the plan of computer networks like distinctive network traffic has shown the self-similar properties.

For instance, packet-switched data patterns and telegraphic engineering traffic flows seem to be present as statistically self-similar. This possession indicates that simple techniques using a Poisson distribution are imprecise networks intended without enchanting self-similarity into concern is probably to function in an unpredicted manner. In the same way, stock market associations are illustrated as exhibiting self-affinity. That is, they come into view self-similar when transformed through a suitable affine transformation intended for the level of the aspect being exposed.

Finite subdivision regulations are powerful techniques used for structuring self-similar sets, including the Sierpinski triangle and the Cantor set. The additional examples of self-similarity are designs on shells, lightning bolts, metal ions or aggregation of bacteria, crystallization patterns in agate, surfaces of cancer cells, quantum particle paths, scores of scaling laws in biology, gamma-ray burst fluctuations, abundances or species distributions, renormalization in quantum electrodynamics, drop formation and so on. We will have various opportunities in the future for our accumulation. Since, further, than any reasonable hesitation, nature is passionate about self-similarity.

3. **Evidence of Self-Similarity in Network Traffic:** (Leland et al., 1994) made a seminal study at AT&T Bell Labs, USA and measured real Ethernet traffic. The pertinent observations are depicted in Fig. 7, from which the following inferences can be made. In Ethernet traffic, no matter what time scale we choose, we shall see similar patterns, unlike the other one. In the case of Ethernet traffic, burstiness exhibits across all time scale, unlike the other one. Hence, network traffic modelling that uses the Poisson process does not take self-similar characteristics in data congestion into consideration. The observable fact of traffic self-similarity has a significant blow on queuing concert and is obtained a major concentration in the network exploring society.

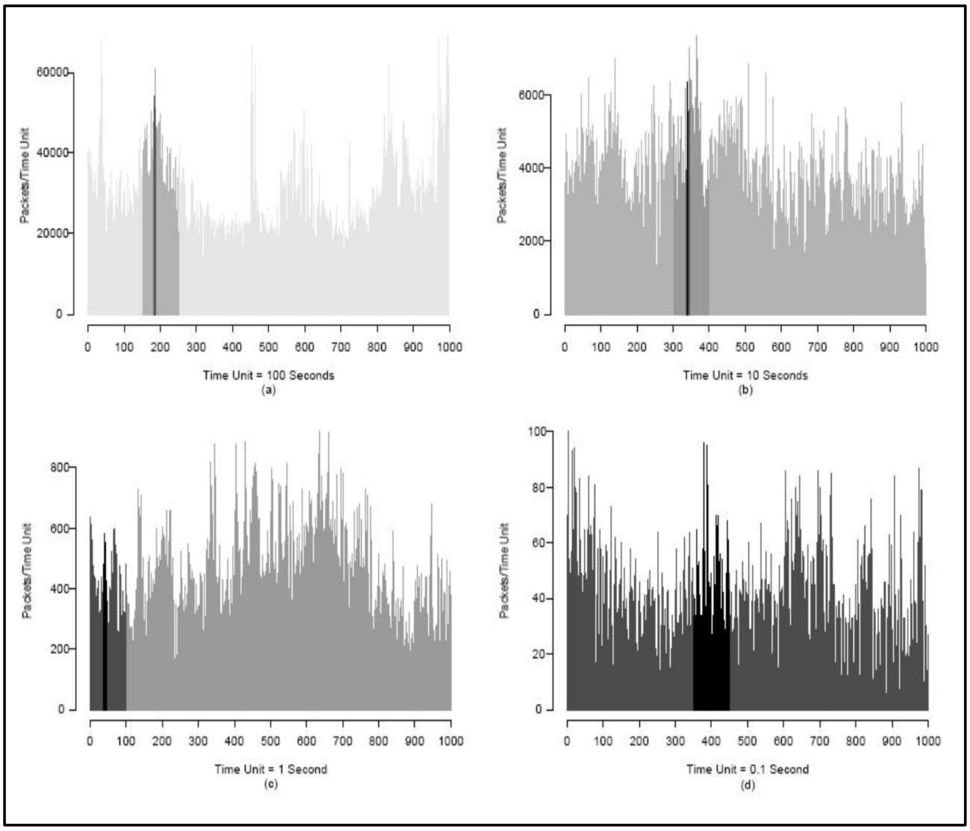

Figure 7: Self-similar nature of Ethernet traffic: Burstiness at various time scales is apparent

Source: Leland et al., 1994

Data networks possess extreme variability (Leland et al., 1994), (Willinger & Paxson, 1998), (Paxson & Floyd, 1995). This variability can be captured by models of LRD. This can be observed from Fig. 8, where traffic means and variance are represented again by the Poisson model and a simple fractal model. The new model exhibits burstiness at different time scales similar to the original traffic. This burstiness is not seen in the Poisson model.

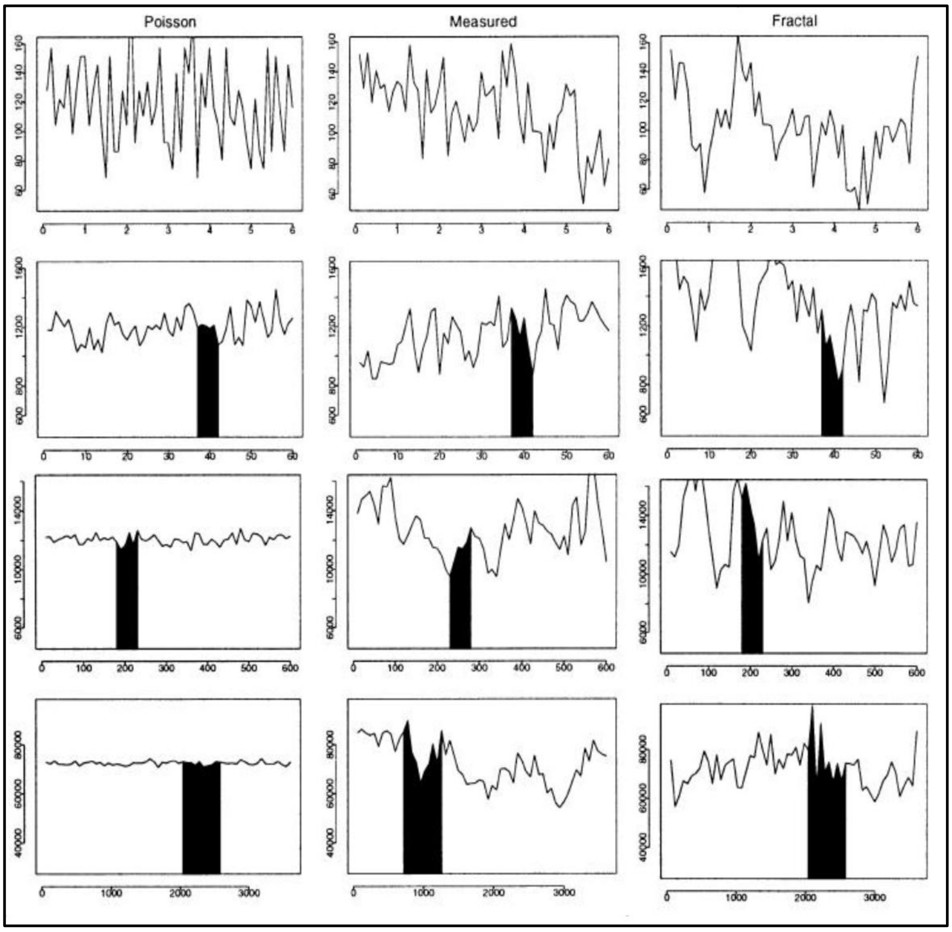

Figure 8: Mean and Variance fit to Synthetized traffic from a Poisson model, Internet traffic and Fractal model over different magnitude

Source: W. Willinger and V. Paxson, 1998

4. **Mathematical Definition of Self-Similarity:** The pioneer of the Self Similar process, Mandelbrot, defined it as a stochastic process whose behaviour is the same at different scales on a dimension (time or space).

   Let $X = \{X_t : t = 1,2,..\}$ be the second-order stochastic process with mean $\mu(constant\ \forall t)$, variance $\sigma^2(constant\ \forall t)$ and ACF $\gamma(s)$ with lag 's' i.e.

   $$\gamma(s) = \frac{Cov(X_t, X_{t+s})}{Var(X_t)}, s \geq 0. \tag{2.7}$$

   Then the aggregating process, $X_t^{(p)}$ is computed using the initial process X_t as

   $$X_t^{(p)} = \frac{1}{p}\sum_{i=1}^{p} X_{(t-1)p+i}\ , t = 1,2, \ldots \tag{2.8}$$

   Where p is an integer (≥ 1) represents the size of blocks for the averaging process.

The ACF of $X_t^{(p)}$ can be given as $\gamma^{(p)}(s)$ as it is also a second-order stationary process.

Definition 1: The A stochastic process $\{X(t), t \geq 0\}$ is known as self-similar if

$$\forall a \geq 0 \, \exists \, b > 0 \, \exists \, X(at) =^d \{bX(t)\} \quad (2.9)$$

where $=^d$ indicates equality of distributions for finite-dimensional and $b = a^H$ where H is the Hurst parameter of the process $X(t)$.

Definition 2: The stochastic process '*X*' is defined to be precisely second-order self-similar with variance σ^2 and Hurst exponent H if

$$\gamma(s) = \frac{\sigma^2}{2}[(s+1)^{2H} - 2s^H + (s-1)^{2H}], \forall s \geq 1 \quad (2.10)$$

Definition 3: The stochastic process '*X*' is defined to be asymptotically second-order self-similar with variance σ^2 and Hurst exponent H if

$$\sum_{m \to \infty} \gamma^{(p)}(s) = \frac{\sigma^2}{2}[(s+1)^{2H} - 2s^H + (s-1)^{2H}], \forall s \geq 1 \quad (2.11)$$

Definition 4: In the variance-time analysis, the process '*X*' is defined to be precisely second-order self-similar with variance σ^2 and Hurst exponent $H = 1 - \frac{\beta}{2}$ if

$$Var\left(X^{(p)}\right) = \sigma^2 p^{-\beta}, \forall p \geq 1 \quad (2.12)$$

From definition one and Eqn. (2.9), we can see that a self-similar process is scale-invariant, i.e. if an entity or object is compiled to subunits continuously on multiple stages, then the subunits at any stage are statistically similar to the considered initial object. Mathematically this property should embrace on all time scales. In real-life situations, there are unavoidably lower and upper bounds over which such self-similar nature apply. Scale invariance is a fundamental property of ensembles of natural images.

5. SRD and LRD

From definition 2 and Eqn. (2.10), we observe that for $H \neq 0.5$

$$\gamma(s) = H(2H-1)s^{2H-2} as \ s \to \infty \quad (2.13)$$

By applying the summation, we get

$$\sum_s \gamma(s) \sim c \sum_s s^{-\beta}, c = H(2H-1) \quad (2.14)$$

The series $c \sum_s s^{-\beta}$ is divergent if $0.5 < H < 1$ or $0 < \beta < 1$ otherwise, it is convergent, being a series of positive terms. The other series $\sum_s \gamma(s)$ can be interpreted accordingly. Thus, for $0.5 < H < 1$, the ACF decays hyperbolically, and the stochastic process *X* is classified as LRD (long-range dependent). And for $0 < H < 0.5$, $\sum_s \gamma(s)$ is finite and the stochastic process *X* is classified as SRD (short-range dependent).

Mathematically, the variation among SRD and LRD process (Cox D.R., 1984) can be stated as follows:

In case of Short-Range Dependence processes, the following properties are identified.

- $E[X_n^p]$ approaches pure noise of second-order as p $\rightarrow\infty$
- For large p, Var[X^p] asymptotically is of the form $\frac{Var[X]}{p}$
- $\sum_{s=0}^{\infty} Cov(X_n, X_{n+s})$is convergent
- S(w) is a spectrum be finite at w =0

In case of Long-Range Dependence processes, the following properties are identified.

- $E[X_n^p]$, as p$\rightarrow\infty$ doesn't approach second-order pure noise
- For large p, Var[X^p] asymptotically is of the form $p^{-\beta}$
- $\sum_{s=0}^{\infty} Cov(X_n, X_{n+s})$ is divergent
- S (w) is a spectrum singular at w =0

IV. METHODS TO ESTIMATE THE HURST PARAMETER OF SELF SIMILAR PROCESS

The Hurst parameter enables us to determine the strength of self-similar behaviour in a time series. H.E. Hurst, a hydrologist, investigated the water storage problems and level patterns regarding the Nile River for several years, and thus the index *H* had emerged. Even though Hurst exponent is mathematically well defined, it's complicated to determine for a given time series.

To compute the Hurst exponent for a small-sized time series, the observations must be taken at high lags. The range of the index *H* is $0 < H < 1$. Many methods are developed in the literature for determining *H* for a time series. Here, we discussed the four widely used methods: R/S method, Variance-time method, Higuchi's method, and Average periodogram method. Finally, we determined the Hurst index *H* for the CPI headline inflation time series using the above methods and compared them.

1. **Rescaled Adjusted Range Statistics (R/S method):** For a self-similar process, the statistical characteristics are invariant with the partition of data. This idea is the sole of this method, where we determine the Hurst exponent by computing the rescaled range over sub-parts of the main data (Gospodinov & Gospodinova, 2005).

   Initially, the rescaled range is computed for the main time series data ($RSave_0$ = RS_0). Then the time series data is partitioned into two equal parts, and rescaled range is computed, giving rise to RS_0 and RS_1. The partitioning of a section continues as in Fig. 9 unless its subsections have less than 8 data values. For each level, the rescaled range values are averaged, and the Hurst exponent is estimated. The adjusted partial sums for the data $X_1, X_2, \dots, X_n$ is defined as:

$$W_j = (X_1 + X_2 + \dots X_n) - j\overline{X}(n), j = 1,2,3, \dots, n \tag{2.15}$$

where $\overline{X}(n)$ is the sample mean.

The range $R(n)$ and standard deviation $S(n)$ are defined by

$$R(n) = \max(0, W_1, W_2, \dots, W_n) - \min(0, W_1, W_2, \dots, W_n) \tag{2.16}$$

$$S(n) = \sqrt{E(X_i - \mu)^2} \tag{2.17}$$

The rescaled adjusted range is defined by

$$\left(\frac{R}{S}\right) statistics = R(n)/S(n) \tag{2.18}$$

According to the power-law relation of $R(n)/S(n)$, we have

$$E\left[\frac{R(n)}{S(n)}\right] \to cn^H, as\, n \to \infty \tag{2.19}$$

Where c is a positive finite constant and H is Hurst exponent. The robustness of this method is discussed in (Mandelbrot-Wallis, 1969).

<table>
<tr><td colspan="8">RS0</td><td>Rsave0</td></tr>
<tr><td colspan="4">RS0</td><td colspan="4">RS1</td><td>Rsave1</td></tr>
<tr><td colspan="2">RS0</td><td colspan="2">RS1</td><td colspan="2">RS3</td><td colspan="2">RS4</td><td>Rsave2</td></tr>
<tr><td>RS0</td><td>RS1</td><td>RS2</td><td>RS3</td><td>RS4</td><td>RS5</td><td>RS6</td><td>RS7</td><td>Rsave3</td></tr>
</table>

Figure 9: Estimation of the Hurst parameter by R/S method

2. **Variance-Time Method:** This method is developed based on gradually decaying variance features of the self-similar process and its aggregated process. The p-aggregate process of $(X_1, X_2, \dots)$ is given by

$$X^{(p)} = (X_1^{(p)}, X_2^{(p)}, \dots)$$

where

$$X_j^{(p)} = \frac{1}{p}\sum_{i=(j-1)p+1}^{p} X_i, j = 1,2, \dots, \frac{N}{p} \quad p, j \in Z^+ \tag{2.20}$$

The variance of the aggregate process(X^p) is defined as:

$$Var\left(X^{(p)}\right) = \frac{1}{N/p}\sum_{i=1}^{p} (X_i^{(p)} - \overline{X}^{(p)})^2 \tag{2.21}$$

For large values of p, $Var\left(X^{(p)}\right)$ decrease linearly. Thus we get

$$Var(X^p) = Var(X)p^{-\beta} \quad (2.22)$$

By applying log on both sides of the above equation, we get

$$\log\left(Var(X^p)\right) = \log\left(Var(X)\right) - \beta\log(p) \quad (2.23)$$

The value of β can be found by estimating a regression line to the plot of $log\ (Var(X^p))$ against $log(p)$. This plot is defined as a variance-time plot. Small values of *p* should be ignored for regression fitting to increase accuracy. Finally, Hurst exponent can be computed using the relation

$$H = 1 - \frac{\beta}{2} \quad (2.24)$$

3. **Higuchi's Method:** A technique suggested by T. Higuchi (1988) uses

$$L(p) = \frac{n-1}{p^3}\sum_{i=1}^{p}\left[\frac{n-1}{p}\right]^{-1}\sum_{k=1}^{[(n-1)/p]}\left|\sum_{j=i+(k-1)p+1}^{i+kp} X(j)\right| \quad (2.25)$$

Here *p* represents block size, *n* represents the size of time series and [ ] stand for the greatest integer function. For a time series with self-similarity or LRD, we have $E\left(L(p)\right) \sim cp^{H-2}$. Being computationally rigorous, this method's results are more accurate, especially in the case of smaller time series like CPI headline inflation we considered. More details of this method are discussed in (Taqqu et al. 1995, 1996)

4. **The Averaged Periodogram Method:** In this method, the spectral representation is used for a stationary process. The averaged periodogram of the process $\{X_i, i = 1,2, \ldots, n\}$ with Fourier frequency λ is given by

$$\widetilde{F}(\lambda) = \int_0^{\lambda} \tilde{I}(\theta)\, d\theta, \qquad 0 < \lambda \leq \pi \quad (2.26)$$

where

$$\tilde{I}(\lambda) = |\widetilde{w}(\lambda)|^2, \qquad \widetilde{w}(\lambda) = \frac{1}{\sqrt{2\pi n}}\sum_{t=1}^{n}(x_t - \mu)\, e^{it\lambda}. \quad (2.27)$$

In this method, $\widetilde{F}(\lambda)$ is estimated using the Robinson integration technique (Robinson, 1994; Lobato & Robinson, 1996). The first step to determine the Hurst exponent is to calculate periodogram and use the relation $\tilde{I}(\lambda) \propto |\lambda|^{1-2H}$. By plotting periodogram against frequency on a log scale and fitting regression, one can obtain the slope *1-2H*.

V. NUMERICAL RESULTS: HURST PARAMETER OF CPI HEADLINE INFLATION

In this section, we compute the Hurst index value using the methods discussed in section 2.4. Applying the R/S approach, the Hurst parameter value of the CPI inflation series is computed using the rescaled range over sub-parts of the data defined in Eqn. (2.18) and finally using the relation $E\left[\frac{R(n)}{S(n)}\right] \rightarrow cn^H, as\ n \rightarrow \infty$. The Hurst index value obtained by this method is 0.9354. To further confirm the self-similarity behaviour of the CPI inflation series, in Fig. 10, we drew the plot for *H* value against the length of the series considered. The range of *H* values in the plot concludes the self-similarity behaviour of the CPI inflation series.

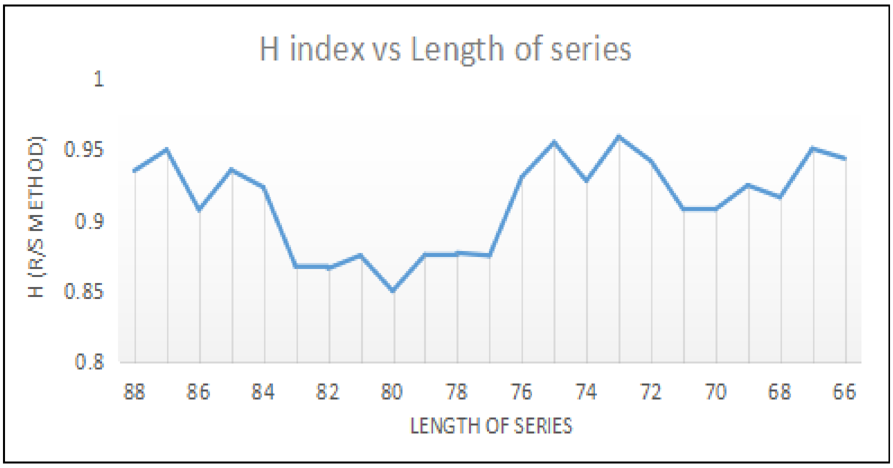

Figure 10: Plot of H index(R/S method) vs Length of series

Table 2.1: Variance-Time values

p	Var(X^p)	log(p)	log(Var(X^p))
2	7.0819	0.301	0.8502
4	6.8767	0.6021	0.8374
8	6.6454	0.9031	0.8226
16	5.5625	1.2041	0.7453
32	5.0262	1.5052	0.7012

In Variance-Time method, the value of H can be found by estimating a regression equation to the plot of $log\,(Var(X^p))$ against $log(p)$ and using the relations $Var(X^p) = Var(X)p^{-\beta}$and $H = 1 - \frac{\beta}{2}$ where $Var(X^p)$ is defined in Eqn. (2.23). The computed values of Variance-time are presented in Table 2.1, and from Fig. 11 of the Variance-time plot, the Hurst index value is obtained as 0.9578. In Fig. 12, we show the *H* index values computed using the Variance-Time technique against the length of the series. The range of the plot concludes the presence of self-similar behaviour in the CPI inflation series.

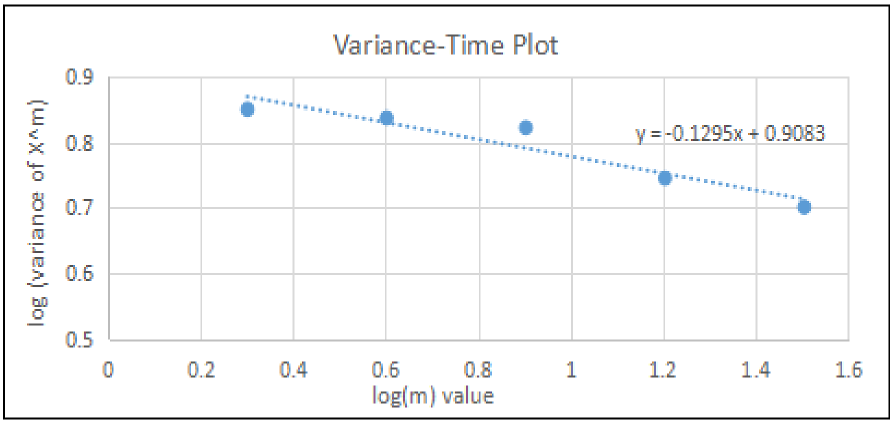

Figure 11: Variance-Time plot for calculating H value

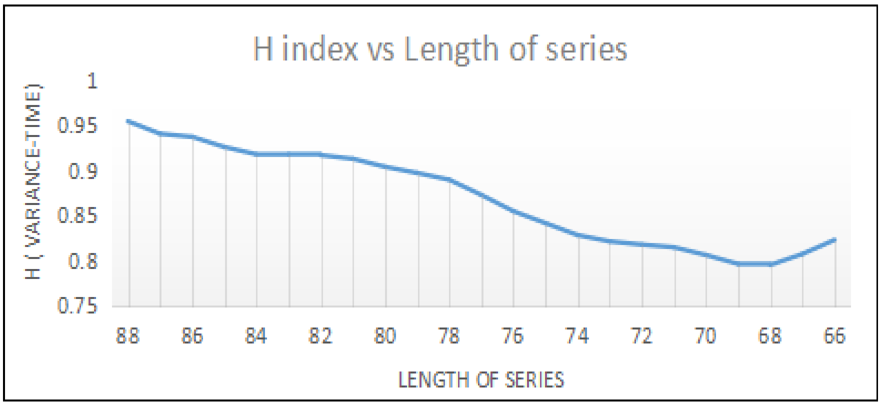

Figure 12: Plot of H index (Variance-Time method) vs Length of series

Table 2.2: Higuchi-Time values

p	L(p)	log(p)	log(L(p))
2	261.45	0.301	2.4174
4	131.08	0.6021	2.1175
8	65.628	0.9031	1.8171
16	32.441	1.2041	1.5111
32	15.627	1.5052	1.1939

In the Higuchi method, we compute $L(p)$ which is defined in Eqn. (2.25), and use the relation $E\left(L(p)\right) \sim cp^{H-2}$ to obtain the Hurst index value. The initial computed values of Higuchi-time are presented in Table 2.2 and then log $\left(L(p)\right)$ is plotted against log (p) in Fig. 13, Higuchi-time plot. Thus, from the graph, the Hurst index value is obtained as 0.9857. In Fig. 14, we present the *H* index values computed using the Higuchi method vs the length of the series. The range of the plot concludes the existence of self-similar behaviour in the CPI inflation series.

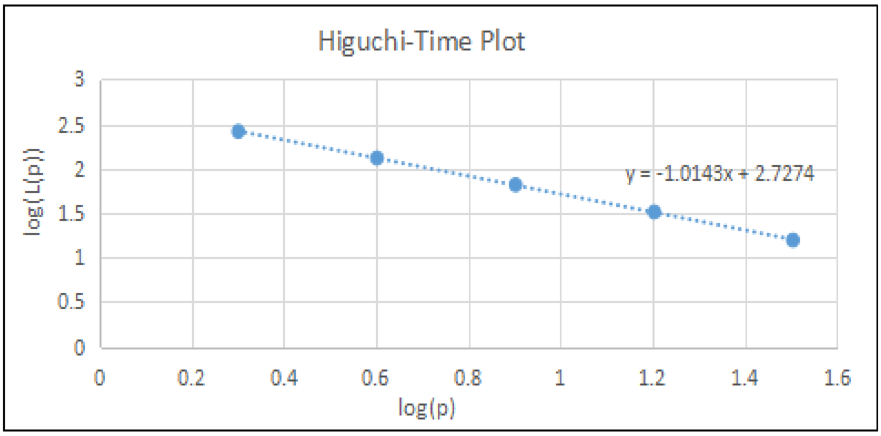

Figure 13: Higuchi-Time plot for calculating H value

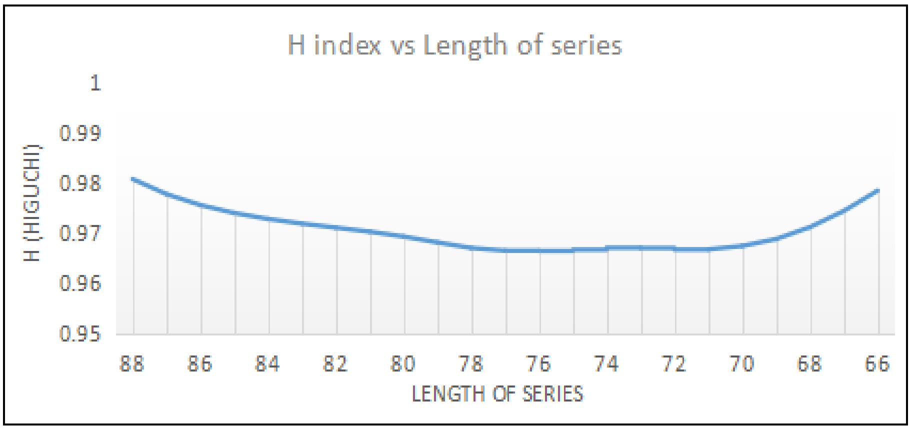

Figure 14: Plot of H index (Higuchi method) vs Length of series

Figure 15: Plot of H index (Robinson-Periodogram method) vs Length of series

In the averaged periodogram method, spectral representation defined in Eqns. (2.26) and (2.27) are used in estimating the Hurst index value. Using the relation $\tilde{I}(\lambda) \propto |\lambda|^{1-2H}$ Hurst index value of CPI headline inflation is obtained as 0.9844. In Fig. 15, we present the H index values computed using the Robinson-Periodogram method vs the length of the series. The plot range suggests that the CPI inflation series has self-similar nature.

All the four widely used methods: R/S method, Variance-time method, Higuchi's method, and Average periodogram method result in Hurst index value which lies in (0.5, 1). All the Hurst index estimates are near to each other and greater than 0.9. This states that the CPI headline inflation time series satisfies the self-similarity and LRD property.

VI. CRITERIA FOR CPI CORE INFLATION AND ITS APPLICATION

In this section, we present the criteria for CPI Core Inflation in terms of Hurst parameter and then use it to judge the conventional exclusion measures of CPI. The Hurst index value measures the intensity of LRD of a series, i.e., the larger the Hurst index value, the larger the LRD or persistence nature. The range of Hurst index value for long-range dependence series lies in (0.5, 1). The results in section 2.6 state that the CPI headline inflation series has LRD property. We also know that the CPI core inflation is identified by eliminating the transient price changes from the CPI headline inflation, specifying that the Hurst parameter of the CPI core inflation measure should be greater than that of CPI headline inflation.

Exclusion based indicators are determined by eliminating certain volatile commodities from the headline inflation. The conventional exclusion based indicators widely used in India for CPI inflation are excluding food commodities, excluding energy commodities and excluding food and energy commodities. CPI excluding food eliminates all the commodities under the food group, which weighs 45.85% of the total CPI basket. CPI excluding energy eliminates the energy group commodities, which weighs only 6.84% of the total CPI basket. Whereas CPI excluding food and energy eliminates both food and energy group commodities whose combined weight is 52.7% of the total CPI basket. Table 2.3 presents the other descriptive statistics of CPI exclusion based indicators. While the mean of CPI excluding energy is very close to the CPI headline inflation, the standard deviation and coefficient of variation of CPI excluding food and energy are less compared to other indicators. Fig. 16 presents the time-series graph of CPI exclusion based indicators and CPI headline inflation. One can see that there is no much difference between the charts of CPI headline inflation and CPI excluding energy, which question the core inflation behaviour of the latter.

Generally, the core inflation measure is expected to have the same mean as the headline inflation. This property is usually known as unbiasedness and tested using the t-test. Table 2.4 presents the p-value results of the t-test and from which we can say that all the conventional CPI exclusion indicators obey the unbiasedness property of the core inflation measure. Further, it is expected that errors should be stationary. The differenced series formed by CPI headline inflation and CPI exclusion indicators are examined for stationarity performing PP and ADF tests. The results of both the tests convey that only CPI excluding energy satisfies the stationarity criteria. So, CPI excluding food and CPI excluding food and energy cannot be considered as a measure of CPI core inflation. As we stated, CPI headline inflation has LRD property; we expect the same from the CPI core measure. Also, the Hurst index value of CPI core measure is expected to be greater than that of CPI headline inflation. Next, we computed the Hurst index value using the Variance-Time method for the three CPI exclusion indicators. The CPI excluding energy has the Hurst index value of 0.936, which is lesser than the Hurst index value of CPI headline inflation which is 0.958, and thus it cannot be CPI core inflation measure. Even though the other two indicators satisfy the Hurst index criteria, they already failed in Stationarity criteria. Apart from these, core measures are also expected to fulfil attractor and exogenous property. Thus LRD or self-similar property of CPI headline inflation has simplified the screening for the core measures. All three conventional CPI exclusion based indicators cannot be treated as CPI core measures and a need to develop new CPI exclusion indicators is identified.

Table 2.3: Descriptive Statistics of Exclusion Based Indicators

S.No	Inflation (CPI)	Mean	Standard Deviation	Coefficient of Variation	Weight
1	Headline	5.994	2.701	0.451	100
2	Excluding food	6.071	1.821	0.299	54.14
3	Excluding energy	5.983	2.781	0.465	93.16
4	Excluding food and energy	6.058	1.767	0.292	47.30

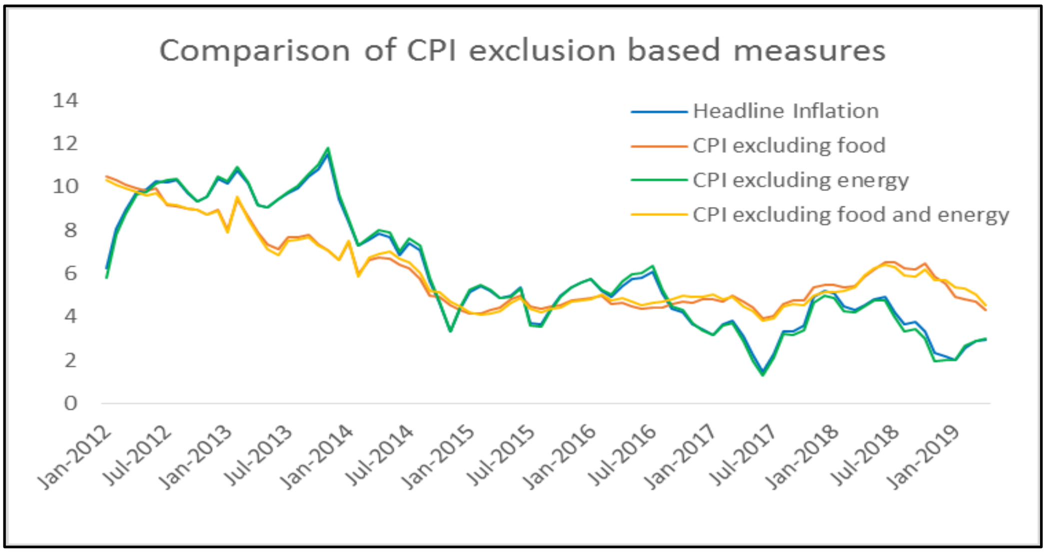

Figure 16: Time series plot to compare CPI exclusion based indicators

Table 2.4: Characteristics of Exclusion Based Indicators

S.No	Core Inflation Indicator (CPI)	Unbiasedness	Stationarity		LRD
		T-Test (P-value)	PP Test (P-value)	ADF Test (P-value)	Hurst Index
1	Excluding food	0.821	0.061	0.133	0.982
2	Excluding energy	0.984	0.043*	0.021*	0.936
3	Excluding food and energy	0.851	0.078	0.154	0.989

*Indicates significance at 0.05 level

Table 2.5: Hurst exponent of CPI inflation at the group level

S.No	Group	Hurst exponent	Weight
1	Food and Beverages	0.885	45.86
2	Pan, tobacco and intoxicants	0.901	2.38
3	Clothing and footwear	0.952	6.53
4	Housing	0.960	10.07
5	Fuel and light	0.927	6.84
6	Miscellaneous	0.969	28.32

Table 2.6: Hurst exponent of CPI inflation at the sub-group level

S.No	Commodity (Sub-group)	Hurst Exponent	Weight
1	Cereals and products	0.894	9.67
2	Meat and fish	0.907	3.61
3	Egg	0.858	0.43
4	Milk and products	0.832	6.61
5	Oils and fats	0.802	3.56
6	Fruits	0.695	2.89
7	Vegetables	0.771	6.04
8	Pulses and products	0.632	2.38
9	Sugar and confectionery	0.132	1.36
10	Spices	0.747	2.5
11	Non-alcoholic beverages	0.9	1.26
12	Prepared meals, snacks, sweets etc.	0.914	5.55
13	Pan, tobacco and intoxicants	0.901	2.38
14	Clothing	0.926	5.58
15	Footwear	0.931	0.95
16	Housing	0.96	10.07
17	Fuel and light	0.927	6.84
18	Household goods and services	0.966	3.8
19	Health	0.872	5.89
20	Transport and communication	0.966	8.59
21	Recreation and amusement	0.81	1.68
22	Education	0.896	4.46
23	Personal Care and Effects	0.808	3.89

VII. HURST PARAMETER OF GROUPS AND SUB-GROUPS OF CPI INFLATION

In the previous section, we identified the need to develop new exclusion-based CPI core inflation as the conventional CPI core inflation indicators fail to satisfy the properties of core inflation. First, we start by examining the Hurst exponent of CPI inflation at the group level. The variance-Time method is used in determining the Hurst exponent. Among the six groups, the ‘food and beverages’ group has the least Hurst exponent indicating less persistence in its series than the other groups (Table 2.5). When this group is excluded, i.e. CPI excluding food indicator attains good persistence with the Hurst exponent of 0.982, but it fails to satisfy other core inflation properties. Additionally, it also leads to the removal of 46% weightage components from the CPI-India basket. The group 'fuel and light' has the Hurst exponent of 0.927, which implies that this group inflation is more persistent than the 'food and beverages' group.

Further, we determined the Hurst exponent of sub-groups (commodities) of the CPI-India basket in Table 2.6. The subgroups: 'sugar and confectionery', 'pulses and products', 'fruits', 'spices' and 'vegetables' have Hurst exponent less than 0.8. Many factors like weight, volatility, correlation with headline and persistence of commodity (sub-groups) inflation influence the CPI headline inflation. Thus a detailed study regarding commodity (sub-group) inflation is carried out, and a new exclusion based core inflation is determined in chapter III.

VIII. CONCLUSIONS

In this chapter, CPI headline inflation is studied for self-similarity behaviour by determining the Hurst index. Various approaches of computing the Hurst parameter have been conversed and applied to CPI headline inflation. The Hurst parameter estimates confirm the presence of self-similar and LRD nature in CPI headline inflation. A criterion for core inflation measures in terms of Hurst exponent is presented. This kind of analysis is beneficial to CPI headline inflation, especially for identifying the CPI core inflation. Mainly, the Hurst index criteria help in identifying the potential core inflation measure from a pool of indicators. The analysis also advises to perform ARFIMA modelling to forecast CPI inflation.

REFERENCES

[1] Baciu, I. C. (2015). Measures of Core Inflation Used by the National Bank of Romania. CES Working Papers, 7(1), 17-30.
[2] Baillie, R. T., & Morana, C. (2012). Adaptive ARFIMA models with applications to inflation. Economic Modelling, 29(6), 2451-2459. doi: 10.1016/j.econmod.2012.07.011
[3] Reddy, D. M., Dasari, R., Perati, M. R., & Reddy, M. K. (2015). Delay behaviour of internet router under self-similar traffic via rational approximations. International Journal of Communication Networks and Distributed Systems, 14(2), 134-144.
[4] Perati, M. R., Kumar, L. R., & Reddy, D. M. (2011). Approximate Markovian model for delay behavior of internet router under self–similar traffic input. Journal of Interdisciplinary Mathematics, 14(3), 321-329.
[5] Perati, M. R., Kumar, L. R., Reddy, D. M., & Kumar, K. S. (2011). Performance Analysis of Internet Router Employing Partial Buffer Sharing Mechanism under Markovian Modelled Self-Similar Variable Packet Length Input Traffic. International Journal of Pure and Applied Mathematics, 67(4), 407-421.
[6] Perati, M. R., Raghavendra, K., Koppula, H. R., Doodipala, M. R., & Dasari, R. (2012). Self-Similar behavior of highway road traffic and performance analysis at toll plazas. Journal of transportation engineering, 138(10), 1233-1238.
[7] Bicchal, M. and Sharma, N. Measuring core inflation in India: An asymmetric trimmed mean approach. Paper presented at 13th Annual Conference on Money and Finance in the Indian Economy, IGIDR. February25–26. Mumbai, India.
[8] Chen, C. C., & Miikkulainen, R. (2001, July). Creating melodies with evolving recurrent neural networks. In IJCNN'01. International Joint Conference on Neural Networks. Proceedings (Cat. No. 01CH37222) (Vol. 3, pp. 2241-2246). IEEE.
[9] Cont, R. (2005). Long range dependence in financial markets. In: Lévy-Véhel J., Lutton E. (eds) Fractals in Engineering. Springer, London. 159-179. https://doi.org/10.1007/1-84628-048-6_11.
[10] Danaee, P., Ghaeini, R., & Hendrix, D. A. (2017). A deep learning approach for cancer detection and relevant gene identification. In Pacific symposium on biocomputing 2017 (pp. 219-229).

[11] Gospodinov, M., & Gospodinova, E. (2005, June). The graphical methods for estimating hurst parameter of self-similar network traffic. In Proceedings of the 2005 International Conference on Computer Systems and Technologies (pp. 1-6). ACM.
[12] Joarder, R. A., Parveen, S., Sarwar, H., Sanyal, S. K., & Rafique, S. (2008, December). Analysis of real-time multimedia traffic in the context of self-similarity. In Proceedings of International Conference on Electrical and Computer Engineering (pp. 618-623). IEEE.
[13] Krishna, T. V., Reddy, D. M., & Rajendar, M. (2020, July). A study on exclusion based measure of core inflation for India. In AIP Conference Proceedings (Vol. 2246, No. 1, p. 020093). AIP Publishing LLC.
[14] Li, X., Lu, H., & Lu, H. (2013, September). QoS analysis of self-similar multimedia traffic with variable packet size in wireless networks. In 2013 IEEE 78th Vehicular Technology Conference (VTC Fall) (pp. 1-5). IEEE.
[15] Liu, J., Shu, Y., Zhang, L., Xue, F., & Yang, O. W. (1999, May). Traffic modeling based on FARIMA models. In Engineering Solutions for the Next Millennium. 1999 IEEE Canadian Conference on Electrical and Computer Engineering (Cat. No. 99TH8411) (Vol. 1, pp. 162-167). IEEE.
[16] Mishkin, F. S. (2007, October). Headline versus core inflation in the conduct of monetary policy. In Business Cycles, International Transmission and Macroeconomic Policies Conference, HEC Montreal, Montreal, Canada.
[17] Sarla, P., Reddy, D. M., & Dingari, M. (2015). A Study on Self Similarity Analysis of Web Users Data at Selected Web Centers. In Proceedings of International conference on Mathematics ICM.